Journal of Alloys and Compounds 509 (2011) L232–L235

Contents lists available at ScienceDirect

Journal of Alloys and Compounds

journal homepage: www.elsevier.com/locate/jallcom

Letter

Synthesis of WO_3 nanoparticles for photocatalytic O_2 evolution by thermal decomposition of ammonium tungstate loading on g-C_3N_4

Hongjian Yan*, Xiaojun Zhang, Shiqing Zhou, Xionghui Xie, Yulai Luo, Yihan Yu

College of Chemistry, Sichuan University, Chengdu 610064, PR China

ARTICLE INFO

Article history:
Received 3 January 2011
Received in revised form 20 March 2011
Accepted 30 March 2011
Available online 6 April 2011

Keywords:
Nanomaterials
Semiconductors
Photocatalysts
Tungsten trioxide

ABSTRACT

Tungsten trioxide (WO_3) nanoparticles have been successfully synthesized by thermal decomposition of ammonium tungstate loading on g-C_3N_4. The as prepared nanoparticles were characterized by XRD, UV–vis, photoluminescence spectra (PL) and TEM. The XRD results indicate that the g-C_3N_4 decomposed completely with WO_3 remaining at calcination temperature higher than 550 °C. The WO_3 prepared at temperature below 750 °C exhibits orthorhombic phase, and monoclinic phase at temperature higher than 850 °C. The UV–vis absorption onset wavelength of the obtained samples is approximately 470 nm, and the absorption intensity increases with calcination temperature, and reaches a maximum at 750 °C. The as prepared WO_3 powders, loaded with 0.5 wt% Pt as cocatalyst, were used as photocatalysts for O_2 evolution from an aqueous KIO_3 solution. The WO_3 nanoparticles prepared from ammonium tungstate loading on g-C_3N_4 showed photocatalytic activity in O_2 evolution up to 77 times higher than that of WO_3 samples prepared from ammonium tungstate without loading on g-C_3N_4.

1. Introduction

Nanomaterials, such as nanoparticles, nanorods, nanowires and nanoribbons, have been of great interest in materials science over a considerable period of time on the basis of their fundamental properties and practical applications in numerous areas. Among various nanomaterials, tungsten oxide (WO_3), an important semiconductor material with a wide band gap ranging from 2.4 to 2.8 eV [1], has attracted considerable interest because of its potential applications in smart windows [2], semiconductor gas sensors [3], solar energy devices [4], optical displays [5] and photocatalysts [6–8] due to its outstanding electrochromic, gaschromic, thermochromic and optochromic properties. Recently, the photocatalytic O_2 evolution on WO_3 from water in the presence of appropriate sacrificial agent has drawn increasing attention [9,10]. The photocatalytic O_2 evolution is a half reaction of stoichiometric water decomposition. Therefore, WO_3 has also been used to construct the Z-scheme system for overall water splitting [11–14]. However, commercially available WO_3 powders were used in these studies. It is well known that the particle size of the photocatalysts plays an important role in the catalytic activity. Therefore, it is essential to synthesize WO_3 with nanostructures. Several synthetic methods, including wet chemistry method [15–17], chemical or physical vapor deposition [18], irradiation method [19] and spray pyrolysis method [20] have been reported to fabricate tungsten oxide with nanostructures. Very recently, nanostructured WO_3 were prepared by an in situ polymerization method using aryl methanol derivative and WCl_6 as starting materials [21].

In this work, tungsten trioxide nanoparticles were prepared by a new method, i.e. the ammonium tungstate was firstly loaded on g-C_3N_4 by impregnation method and then calcined at high temperature. The results indicated that the g-C_3N_4 decomposed completely and only WO_3 nanoparticles remaining at calcination temperature higher than 550 °C. The as prepared WO_3 powders, loaded with 0.5 wt% Pt as cocatalyst, were used as photocatalysts for O_2 evolution from an aqueous KIO_3 solution. The WO_3 nanoparticles showed photocatalytic activity in O_2 evolution up to 77 times higher than that of WO_3 samples prepared from ammonium tungstate without loading on g-C_3N_4.

2. Experimental

All the reagents were of analytical grade, and were used without further purification. The g-C_3N_4 powder was prepared by directly heating melamine at 600 °C for 4 h under a flow of Ar gas according our previous method [22].

WO_3 nanoparticles were prepared by calcination the ammonium tungstate loading on the surface of g-C_3N_4. In a typically process, ammonium tungstate (1.0 g) was dissolved in distilled water (20 mL). Then 1.0 g of as prepared g-C_3N_4 was added to the ammonium tungstate solution under vigorous stirring. After stirred for overnight the water was evaporated to get yellowish powder, and then calcined the powder in air at different temperatures for 2 h.

The structural properties of the products were analyzed by X-ray powder diffraction (XRD) on a X-Pert Pro diffractometer with CuKα radiation ($\lambda = 1.5406$ Å) at a scanning speed of 4° min^{-1}. UV–vis diffuse reflection spectra were measured using a UV–vis spectrophotometer (UV2100, Shimadzu) and converted from reflection to

---

* Corresponding author. Tel.: +86 28 85221339; fax: +86 28 85221339.
E-mail address: hjyan@scu.edu.cn (H. Yan).

0925-8388/$ – see front matter © 2011 Elsevier B.V. All rights reserved.
doi:10.1016/j.jallcom.2011.03.181

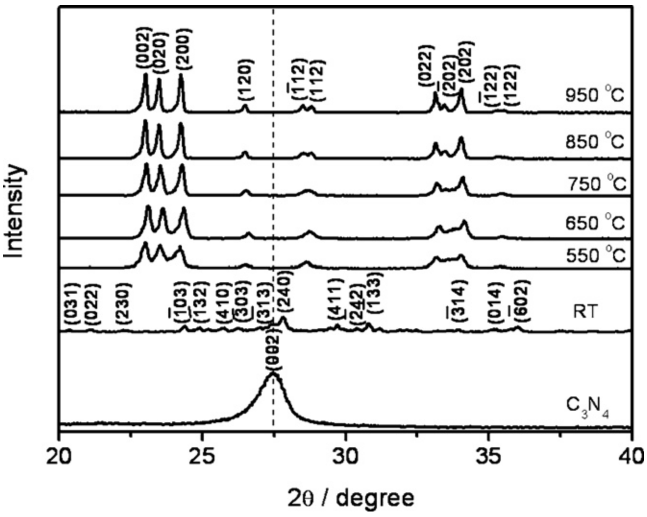

Fig. 1. XRD patterns of WO_3 prepared at different temperatures.

absorbance by the Kubelka–Munk method. The photoluminescence measurements were performed in a luminescence spectrophotometer (Hitachi F-7000) operated at room temperature. The morphology of the products was characterized by using JEM-100CX Transmission Electron Microscope (TEM, JEOL, Japan).

The loading of Pt cocatalyst on WO_3 was performed by impregnation method. 0.3 g of WO_3 powder was impregnated in an aqueous solution containing a certain amount of H_2PtCl_6. The solution was then evaporated over a water bath at 80 °C followed by calcination in air at 500 °C for 1 h.

The photocatalytic reaction was carried out in an inner irradiation quartz cell (500 mL). The reaction cell was connected to a closed gas circulation system and the gases evolved were analyzed with an on-line TCD gas chromatograph (SPSIC, GC-102AT, argon carrier). In a typically photocatalytic reaction, 0.3 g of WO_3 powder, loaded with 0.5 wt% Pt, was suspended in 500 mL of aqueous KIO_3 solution (5 mmol dm^{-3}) under magnetic stirring. The reaction vessel was evacuated several times to completely remove the air. The mixture was then irradiated with light from a 300 W high pressure mercury lamp. The temperature of the reaction medium was maintained at 298 K by a flow of cooling water during the reaction.

3. Results and discussion

The crystalline phases of the samples before and after calcination at different temperatures were characterized by XRD. As shown in Fig. 1, the peak at $2\theta = 27.4°$ can be indexed to (0 0 2) diffraction plane of the graphite-like C_3N_4 [22,23]. The structure of g-C_3N_4 was still maintained after loaded with ammonium tungstate on its surface. XRD patterns from the sample clearly show that the powder before calcination presents a two-phase composition of g-C_3N_4 and ammonium tungsten oxide (JCPDS 71-2433). The diffraction peak of g-C_3N_4 disappears and only the peaks of WO_3 remain after calcination the samples at temperature higher than 550 °C, which indicates that the g-C_3N_4 decomposed completely. It is reported that tungsten trioxide exists in several polymorph phases: orthorhombic, triclinic, monoclinic, tetragonal and hexagonal [24]. The orthorhombic WO_3 phase characteristically exhibits three intense peaks at $2\theta = 23.1°$, 23.6°, and 24.4°. However, the monoclinic WO_3 phase characteristically exhibits three intense peaks at $2\theta = 23.1°$, 23.6°, and 24.4° and twin peaks in the ranges 28–30°, 35–36°. Therefore, the XRD patterns shown in Fig. 1 demonstrate the WO_3 samples calcination below 750 °C exhibits orthorhombic phase (JCPDS 20-1324), and the samples calcinations higher than 850 °C exhibits monoclinic phase (JCPDS 43-1035). The XRD result also indicates that all WO_3 samples were well crystallized. The XRD results in Fig. 1 also reveal changes in the peak intensities of the obtained samples with temperature. The diffraction peaks became sharper with increasing calcination temperature, which indicates that the crystallinity of WO_3 becomes higher with increasing calcination temperature. The effect of the calcination temperature on the crystallite dimensions of WO_3 was also detected by XRD. The average crystal size of WO_3 was estimated by using the Scherrer equation [25]:

$$D = \frac{K\lambda}{\beta \cos\theta}$$

where D is the crystalline size, K is the so-called shape factor and usually taken as 0.89, λ and θ are the radiation wavelength and Bragg's angle, respectively, β is the full width at half maximum (FWHM) of the diffraction peak. The average grain size

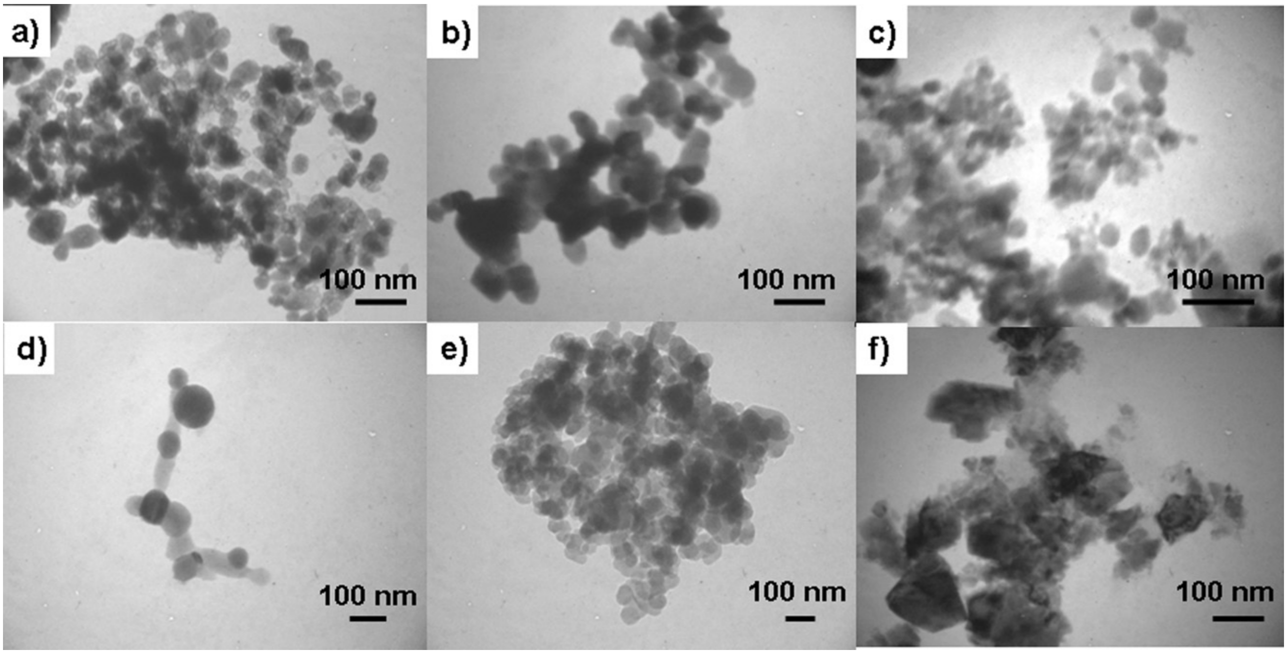

Fig. 2. The TEM images of WO_3 prepared by calcinations ammonium tungsten loading on C_3N_4 at 550 °C (a), 650 °C (b), 750 °C (c), 850 °C (d), 950 °C (e) and from ammonium tungsten without loading on C_3N_4 at 750 °C (f).

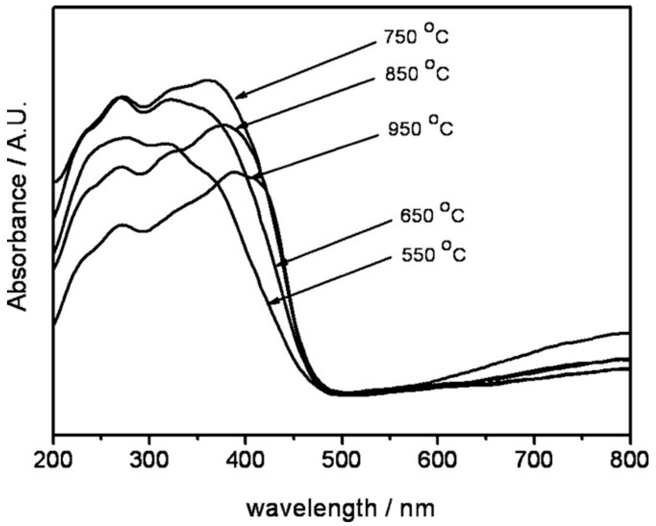

Fig. 3. UV–vis absorption spectra of as prepared WO_3 samples.

of WO_3 obtained at 550 °C, 650 °C, 750 °C, 850 °C and 950 °C is 58 nm, 69 nm, 80 nm, 106 nm and 114 nm, respectively, indicating that the grain size of as prepared WO_3 grew up with calcinations temperature.

Fig. 2 shows the TEM images of the WO_3 samples obtained at different temperatures. It can be seen from Fig. 2a–e, the spherical shaped WO_3 could be obtained by calcination the ammonium tungstate loading on g-C_3N_4. The particle size of the products is in agreement with the results of XRD and increases with heat-treatment temperature increasing. However, the significant change of morphology for WO_3 samples took place when calcination ammonium tungstate without loading on g-C_3N_4, forming the irregular and un-uniform shape (Fig. 2f). It could also be observed that the particle size of WO_3 prepared by decomposition ammonium tungstate without loading on g-C_3N_4 was ranging from 50 to 200 nm.

The UV–vis spectra of the WO_3 samples are shown in Fig. 3. The absorption onset wavelength of the obtained samples is approximately 470 nm, and the band gap value of as synthesized WO_3 is 2.6 eV, as calculated from following formula: $E_g = 1240/\lambda$. The absorption intensity of the WO_3 samples increases with calcination temperature, and reaches a maximum at 750 °C.

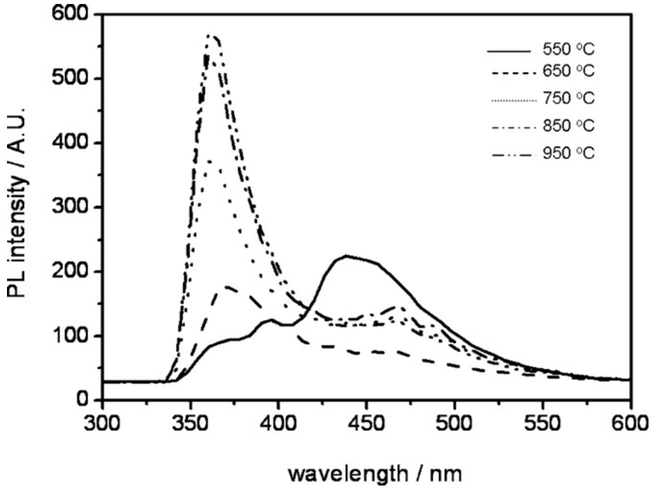

Fig. 4. Room-temperature photoluminescence spectra of as prepared WO_3 samples.

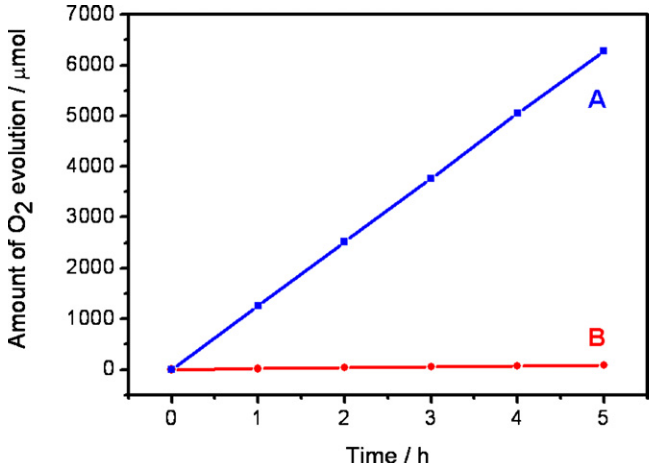

Fig. 5. The amount of photocatalytic O_2 evolution on WO_3 prepared by calcination ammonium tungstate loading on g-C_3N_4 (A) and without loading on g-C_3N_4 (B) at 750 °C.

Fig. 4 shows the room temperature photoluminescence spectra of the WO_3 samples obtained at different temperatures. When excited at 231 nm, two emission bands in the spectra of WO_3 calcination at temperature higher than 650 °C are observed including the UV emission with the center wavelength at 361 nm and the blue emission with the center wavelength at 468 nm, while three emission bands (centered at around 361 nm, 393 nm and 439 nm, respectively) in the spectra of WO_3 calcination at 550 °C are observed. The blue emission is attributed to band-band indirect transition of the bulk phase WO_3 and the UV emission is due to the localized state of oxygen vacancies in WO_3 [26].

Fig. 5A and B shows the photocatalytic O_2 evolution on WO_3 prepared by calcination ammonium tungstate with and without loading on g-C_3N_4 at 750 °C from water containing 0.005 M $IO_3{}^-$ as electron acceptors, respectively. The rate of O_2 evolution on WO_3 prepared from ammonium metatugsten without loading on g-C_3N_4 was about 16.2 μmol h^{-1}. However, the rate of O_2 evolution on WO_3 calcination at 750 °C is about 1256.3 μmol h^{-1}. The activity of WO_3 in O_2 evolution increased by up to 77 times, comparing to that of WO_3 sample prepared from ammonium tugstate without loading on g-C_3N_4. The calcination temperature had effect on the rate of photocatalytic O_2 evolution. As shown in Fig. 6, tungsten trioxide samples obtained at 750 °C exhibited the highest activity for O_2 evo-

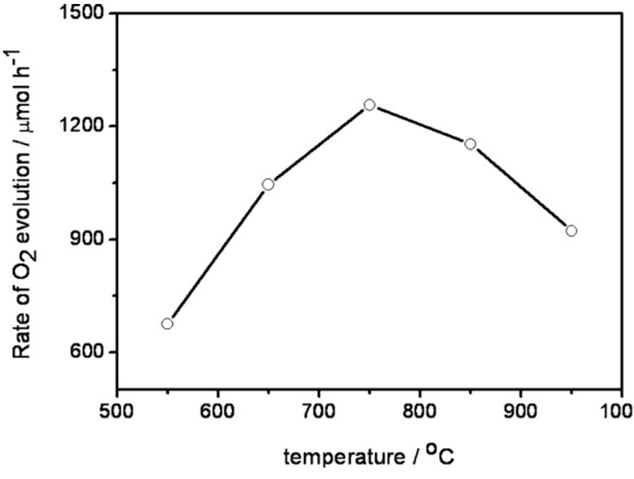

Fig. 6. Rate of O_2 evolutions under light irradiation in a 5 mM aqueous KIO_3 solution as a function of calcinations temperature.

lution. The maximum photocatalytic activity may be attributed to the maximum absorption intensity as shown in the UV–vis spectra (Fig. 3).

4. Conclusions

In summary, WO_3 nanoparticles with an average diameter of approximately 50–120 nm have been successfully synthesized by thermal decomposition of ammonium tungstate loading on g-C_3N_4. The XRD results indicate that the g-C_3N_4 decomposed completely with WO_3 remaining at calcination temperature higher than 550 °C. The WO_3 prepared at temperature below 750 °C exhibits orthorhombic phase, and monoclinic phase at temperature higher than 850 °C. The UV–vis absorption onset wavelength of the obtained samples is approximately 470 nm, and the absorption intensity increases with calcination temperature, and reaches a maximum at 750 °C. The as prepared WO_3 powders, loaded with 0.5 wt% Pt as cocatalyst, were used as photocatalysts for O_2 evolution from an aqueous KIO_3 solution. The WO_3 nanoparticles prepared from ammonium tungstate loading on g-C_3N_4 showed photocatalytic activity in O_2 evolution up to 77 times higher than that of WO_3 samples prepared from ammonium tungstate without loading on g-C_3N_4.

Acknowledgements

We thank the Fundamental Research Funds for the Central Universities (Project No. 2009SCU11105) and Dalian Institute of Chemical Physics (Prof. Can Li) for the financial support. We also thank Sichuan University Analytical & Testing Center for TEM (Y. He and S.P. Zheng), PL and XRD analysis.

References

[1] S.M. Sun, W.Z. Wang, S.Z. Zeng, M. Shang, L. Zhang, J. Hazard. Mater. 178 (2010) 427–433.
[2] S.H. Wang, T.C. Chou, C.C. Liu, Sens. Actuators B 94 (2003) 343–351.
[3] S. Supothina, P. Seeharaj, S. Yoriya, M. Sriyudthsak, Ceram. Int. 33 (2007) 931–936.
[4] C.G. Granqvist, Sol. Energy Mater. Sol. Cells 60 (2000) 201–262.
[5] C.G. Granqvist, Handbook of Inorganic Electrochromics Materials, Elsevier, Amsterdam, 1995.
[6] R. Abe, H. Takami, N. Murakami, B. Ohtani, J. Am. Chem. Soc. 130 (2008) 7780–7781.
[7] A. Sclafani, L. Palmisano, G. Marcí, A.M. Venezia, Sol. Energy Mater. Sol. Cells 51 (1998) 203–219.
[8] T. Arai, M. Yanagida, Y. Konishi, Y. Iwasaki, H. Sugihara, K. Sayama, J. Phys. Chem. C 111 (2007) 7574–7577.
[9] K. Sayama, H. Arakawa, J. Phys. Chem. 97 (1993) 531–533.
[10] W. Erbs, J. Desilvestro, E. Borgarello, M. Grätzel, J. Phys. Chem. 88 (1984) 4001–4006.
[11] G.R. Bamwenda, H. Arakawa, Sol. Energy Mater. Sol. Cells 70 (2001) 1–14.
[12] H. Kominami, K. Yabutani, T. Yamamoto, Y. Kera, B. Ohtani, J. Mater. Chem. 11 (2001) 3222–3227.
[13] R. Abe, T. Takata, H. Sugihara, K. Domen, Chem. Commun. (2005) 3829–3831.
[14] K. Maeda, M. Higashi, D. Lu, R. Abe, K. Domen, J. Am. Chem. Soc. 132 (2010) 5858–5868.
[15] X.L. Li, J.F. Liu, Y.D. Li, Inorg. Chem. 42 (2003) 921–924.
[16] P. Judeinstein, J. Livage, J. Mater. Chem. 1 (1991) 621–627.
[17] O. Lev, Z. Wu, S. Bharathi, V. Glezer, A. Modestov, J. Gun, et al., Chem. Mater. 9 (1997) 2354–2375.
[18] Y. Baek, K. Yong, J. Phys. Chem. C 111 (2007) 1213–1218.
[19] A. Rougier, F. Portemer, A. Quédé, M. Marssi, Appl. Surf. Sci. 153 (1999) 1–9.
[20] R. Hurdich, Electron. Lett. 11 (1975) 142–144.
[21] F.B. Hiller, R. Lungwitz, A. Seifert, M. Hietschold, M. Schlesinger, M. Mehring, S. Spange, Angew. Chem. Int. Ed. 48 (2009) 8878–8881.
[22] H. Yan, H. Yang, J. Alloys Compd. 509 (2011) L26–L29.
[23] S. Matsumoto, E.Q. Xie, F. Izumi, Diamond Relat. Mater. 8 (1999) 1175–1182.
[24] G. Xin, W. Guo, T.L. Ma, Appl. Surf. Sci. 256 (2009) 165–169.
[25] R. Jenkins, R.L. Snyder, Chemical Analysis: Introduction to X-ray Powder Diffractometry, John Wiley & Sons, Inc., New York, 1996.
[26] J.Y. Luo, F.L. Zhao, L. Gong, H.J. Chen, J. Zhou, Z.L. Li, et al., Appl. Phys. Lett. 91 (2007) 0931241–931243.